

Ultrafast relaxation dynamics of optically excited electrons in Ni_3^- N. Pontius, M. Neeb, and W. Eberhardt
*BESSY GmbH, Albert-Einstein-Straße 15, 12489 Berlin, Germany*G. Lüttgens and P. S. Bechthold
Institut für Festkörperforschung, Forschungszentrum Jülich GmbH, 52425 Jülich, Germany
(Received 9 August 2002; published 31 January 2003)

Photon-induced ultrafast energy dissipation in small isolated Ni_3^- has been studied by two-color pump-probe photoelectron spectroscopy. The time-resolved photoelectron spectra clearly trace the path from a single-electron excitation to a thermalized cluster via both inelastic electron-electron scattering and electron-vibrational coupling. The relatively short electron-electron-scattering time of 215 fs results from the narrow energy spread of the partially filled d levels in this transition-metal cluster. The relaxation dynamics is discussed in view of the cluster size and in comparison to the totally different relaxation behavior of s/p -metal clusters.

DOI: 10.1103/PhysRevB.67.035425

PACS number(s): 33.80.Eh, 36.40.-c, 42.65.Re

I. INTRODUCTION

Electron-scattering processes play a key role for many phenomena in condensed matter physics. Giant magnetoresistance,¹ photon-induced interaction of molecules or atoms with surfaces,² or magneto-optical data storage³ are only a few examples. Approaching the nanometer scale the scattering rate of excited electrons is significantly affected by the size of the physical system. In particular, this becomes evident when the size is reduced to the same dimension as the mean scattering length of an excited electron. Considering the proceeding miniaturization of electronic devices a detailed understanding of electron-scattering processes is thus not only of fundamental interest but also of great technological importance.

If an electron in a bulk metal is excited about 1 eV or more above the Fermi level, the predominant relaxation process is inelastic electron-electron scattering. The mean scattering time τ_{e-e} usually amounts to a few tens of femtoseconds.⁴⁻⁶ τ_{e-e} considerably depends on the density of states (DOS) around the Fermi level (E_F) which is generally large and continuous in metals. Moreover, in transition metals the DOS around E_F is considerably enhanced by d states. Therefore the lifetime of excited electrons in d metals is typically about one order of magnitude smaller than in noble metals.

The size dependence of electron relaxation processes has been investigated in nanoparticles down to a diameter of 4 nm.⁷⁻¹⁰ For silver nanoparticles from about 30 nm to 4 nm diameter the electron-electron scattering time decreases steadily by a factor of 2 (Ref. 10). Here the *spillout* of the conduction electrons leads to a reduced electron screening with decreasing particle size which increases the Coulomb interaction between the scattering electrons.

However, if the size of metallic systems is reduced to the subnanometer scale, the DOS is substantially affected by quantum confinement. This leads to a rather discrete electronic structure. Consequently photoemission spectra of noble and simple metal clusters show sharp and well-separated peaks.¹¹⁻¹³ Thus for an excited electron the prob-

ability of inelastic scattering with other electrons is significantly reduced. Therefore in optically excited small noble and simple metal clusters slow processes like nuclear wave packet dynamics, luminescence, and dissociation on a picosecond or even nanosecond time scale have been observed instead of inelastic electron scattering.¹⁴⁻¹⁶

In contrast, recent time-resolved photoemission studies on small *transition-metal* clusters have demonstrated inelastic electron-scattering processes on a femtosecond time scale.¹⁷⁻¹⁹ Similar to bulk metals the ultrafast relaxations in transition-metal clusters are enabled by the large DOS around the highest occupied molecular orbital (HOMO) which is caused by the partially filled d levels. These d levels create a rather dense electronic level structure in the upper valence region even in very small clusters as discussed in this paper.

We present time resolved data on ultrafast electron relaxations in Ni_3^- measured in a two-color pump-probe experiment. The use of two colors allows for a background-free measurement of the excited electron intensity. The photoelectron data reveal sequential energy-dissipation steps between the initial single-electron excitation and the thermalized cluster i.e., inelastic electron-scattering and electron-vibrational coupling. In contrast to similar experiments on bulk surfaces the number of degrees of freedom and the amount of absorbed energy are exactly known for an isolated gas phase cluster.

II. EXPERIMENT

The experimental setup has been described in detail in Ref. 20. Clusters are produced in a pulsed-laser vaporization source by aggregation of metal vapor in a He carrier gas. A cluster beam is formed in an adiabatic expansion. Anionic clusters are deflected and size selected from the cluster beam by a time-of-flight mass spectrometer. When cluster anions of the desired size enter the magnetic-bottle time-of-flight electron spectrometer they are decelerated and electrons are detached using the pump and probe femtosecond-laser pulse. The pulses are generated in a low-repetition (up to 100 Hz)

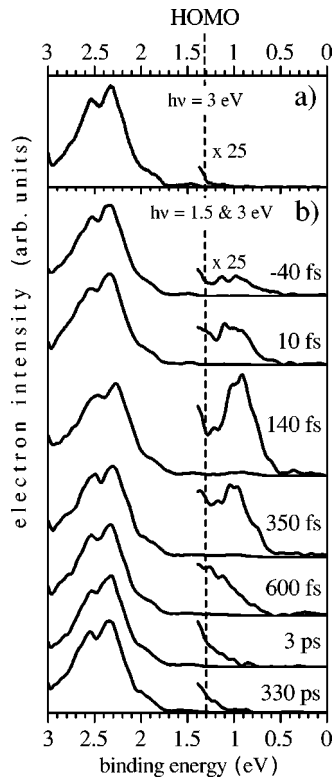


FIG. 1. Femtosecond photoelectron spectra of Ni_3^- taken with fs pulses (80 fs). (a) Single-photon photoemission with 3-eV photons. (b) Time-resolved photoemission spectra using a 1.5-eV pump and a 3-eV probe photon. The rapid changes of the intensity distribution above the HOMO [dotted line at 1.3 eV (Ref. 24)] indicate the ultrafast relaxation of the optically excited electrons by inelastic electron scattering.

oscillator-amplifier Ti:sapphire laser system. The resolution of the electron spectrometer amounts to 30 meV on average. Fundamental (photon energy 1.5 eV, ~ 1 mJ/pulse, temporal width ~ 80 fs) and second-harmonic laser pulses (~ 0.3 mJ/pulse, temporal width ~ 80 fs) of Ti:sapphire have been used in the measurements. In the two-color pump-probe setup the position of zero delay between the pump and probe pulses is determined experimentally via polarization gating in the rear window of the vacuum chamber.

III. RESULTS AND DISCUSSION

Figure 1 shows photoelectron spectra of Ni_3^- taken with fs-laser pulses of 80 fs width. The uppermost spectrum (a) is recorded with fs *single* pulses of 3 eV photon energy and reveals mainly direct photoemission.^{21,22} This spectrum reflects in a good approximation the occupied DOS of Ni_3^- in its electronic ground-state configuration. The small intensity above²³ the HOMO results from two-photon photoemission (2PPE) due to the intense 3 eV femtosecond pulse.

Figure 1(b) displays a series of pump-probe 2PPE spectra of Ni_3^- . These have been recorded using *two* subsequent femtosecond-laser pulses: the pump pulse at 1.5 eV photon energy and the probe pulse at 3 eV photon energy. The temporal delay between the two pulses ranges from

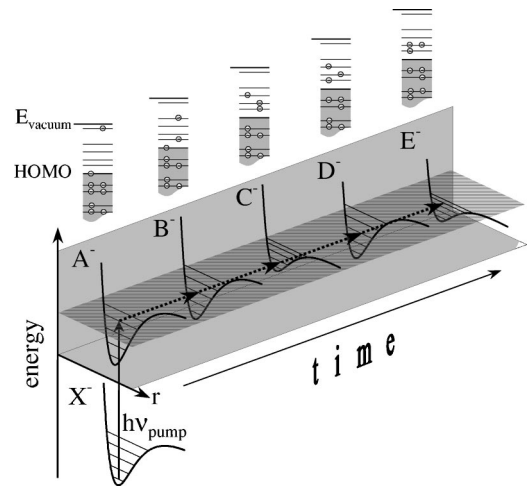


FIG. 2. Scheme of the electron relaxation process via inelastic electron-electron scattering in a simple one-particle picture (upper part) and in terms of transitions between electronic states of a small isolated cluster (lower part).

–40 fs to 330 ps. A significant change of the excited electron intensity (magnified by a factor of 25) is observed at a binding energy below 1.3 eV. With increasing delay a broad peak around 0.9 eV grows in continuously and reaches a maximum at about 140 fs. This initially excited intensity distribution reflects the so-called *joint density of states*.¹⁸ At later times the electron intensity begins to fade while the intensity distribution shifts towards higher binding energies. This indicates a fast relaxation of excited electrons by inelastic electron-electron scattering as is well known from similar experiments on metal surfaces.⁵ At delays larger than 3 ps the spectra remain almost unchanged, showing an exponential-like decreasing intensity distribution.

The inelastic electron-electron scattering is schematically illustrated in the level diagrams in the top of Fig. 2. The optically excited electron scatters with an electron below the HOMO, thereby transferring a fraction of its excitation energy to the scattered counterpart. Due to the Pauli principle, both electrons reside above the HOMO at binding energies larger than the binding energy of the initially excited electron. This induces the observed intensity shift in the electron spectra. Generally the relaxation proceeds in a cascade of many further scattering events, leading to many-electron excited states. After a sufficient number of scattering processes the electron system attains thermal equilibrium obvious by a thermal electron intensity distribution at $\Delta\tau \gtrsim 3$ ps. The subsequent decrease of the *total* intensity is caused by the drain of energy from the electronic into the vibrational system via electron-vibational coupling.

An essential difference between the relaxation processes in a free small cluster with respect to the bulk is the limited number of degrees of freedom. Consequently the total energy (i.e., basically the absorbed photon energy of 1.5 eV) is conserved during the whole relaxation process and remains localized inside an isolated cluster in contrast to macroscopic surfaces where the energy can diffuse into the bulk, e.g., by ballistic transport. Accordingly, it is appropriate to describe the inelastic electron-scattering processes in an isolated par-

title as a series of transitions from one electronic state to another.

Upon interaction with the exciting laser pulse a wave packet is created on the potential energy surface of the excited electronic state A^- . As the excitation process is usually instantaneous compared to nuclear motion the transition occurs vertically in the potential surface diagram. The inelastic scattering of the excited electron results in an electronic transition from state A^- to B^- corresponding to the new electronic level configuration. This causes the wave packet in A^- to develop onto the potential surface of B^- . The time scale of such transitions is determined by the lifetime of the excited electron, τ_{e-e} . Further scattering events succeed by additional transitions into the electronic states C^- , D^- , E^- , etc. The conservation of total energy during the relaxation is accounted for by fixing the position on the energy scale as a function of the time (i.e., the semitransparent plane in Fig. 2). Considering the Heisenberg uncertainty principle and the laser spectral bandwidth the time-dependent cluster state is mainly composed of eigenstates located in the immediate vicinity of this energy plane.

After photoexcitation the nuclei find themselves in an altered Coulomb potential which depends on the particular electronic state of the cluster. Consequently the nuclei are no longer in geometric equilibrium and start to rearrange within the new potential. Hereby the nuclei gain potential and kinetic energy at the expense of the electronic systems energy. In turn, the change of the cluster geometry modifies the electronic structure which vice versa retroacts on the relaxation process. Altogether the relaxation of the excited cluster depends on both electronic and geometric changes. At the end of the dissipation process the electronic and nuclear systems reach thermal equilibrium at an elevated temperature. Depending on this final temperature the nuclei do not just vibrate but may even permanently change their positions which means that the cluster has become liquid.²⁶

From the above consideration it is obvious that the more cluster states are available in the immediate vicinity of the excitation energy, the faster the relaxation via inelastic electron-electron scattering proceeds. To get an idea of the mean number of cluster states per energy interval for a triatomic Ni-like cluster a fictive level scheme is presented in Fig. 3. The electronic level configuration is deduced from a d^9s^1 atomic configuration. The d -level bandwidth is assumed to be 4 eV, similar to the bulk value. This is justified by the fact that the energetic spread of the localized d orbitals is mainly caused by the interaction with the immediate neighbor atoms which has been verified in calculations of the electronic structure of, e.g., Ni_4^- (Ref. 25) or Pd_{13}^-/Pt_{13}^- (Refs. 27 and 28). For the s/p levels a typical bandwidth of 15 eV is supposed. The relative position of d and s/p levels is approximately given by the level occupation in the electronic ground state of the trimer (3 d and 21 s/p levels are unoccupied; 27 d and 3 s/p levels are occupied). The average number of cluster states within a specific total energy range is then derived by systematically combining the occupation of this electronic level scheme. A number of 280 states results within a total energy range between 0 eV, and 1.5 eV, corresponding to a mean value of roughly 20 states per 100 meV.

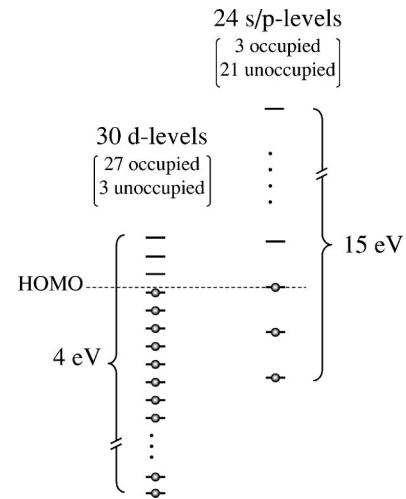


FIG. 3. Level scheme of a triatomic transition-metal cluster. The level occupation is deduced from a d^9s^1 atomic configuration.

It is very instructive to compare this value with that of a triatomic noble or simple metal cluster (e.g., Ag_3 or Na_3). Here the upper valence region is composed of s/p levels only. Combining the occupation of a corresponding electronic level system (3 occupied versus 21 unoccupied s/p levels, no d levels) only three cluster states can be found with a total energy below the excitation energy 1.5 eV. This is two orders of magnitude smaller than in a transition-metal cluster and impressively explains the different relaxation behavior of a transition- and a noble-metal cluster.

From Fig. 2 it becomes evident that the splitting of the electronic states into a series of vibronic sublevels must play an important role for the relaxation process (typical vibrational energies range from 5 meV to 200 meV). The electronic states are not only accessible in the immediate neighborhood of the electronic state, but also in a particular energy interval corresponding to the vibrational broadening. The splitting into vibrational sublevels multiplies the number of possible relaxation pathways and thus enhances the probability of inelastic electron scattering.

The above estimate of the number of states per energy interval only provides an average value of the electronic states' density. In a real cluster the electronic levels are generally not distributed equidistantly and hence the density of cluster states may fluctuate depending on the excitation energy. In consequence, the relaxation behavior of each individual cluster may depend on the individual electronic structure as it determines the number of accessible cluster states in the particular excitation energy range.¹⁸

A qualitative estimate of the unoccupied DOS of Ni_3^- can be deduced from an evaluation of the resonant 2PPE spectrum. Figure 4 displays the pump-probe spectrum at a delay of 140 fs. As already mentioned the intensity distribution above the HOMO reflects in a good approximation the *joint density of states*: $JDOS(E_n, \hbar\omega) := g(E_i) |M_{ni}|^2 g(E_n = E_i + \hbar\omega)$. Here M_{ni} is the dipole matrix element for the resonant transition from the initial state $|i\rangle$ to the intermediate state $|n\rangle$ and $g(E)$ corresponds to the level density. In this approximation any relaxation is neglected (see deduced elec-

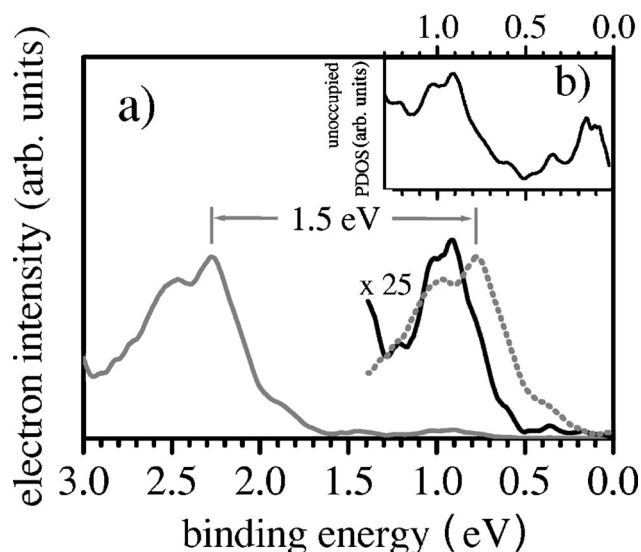


FIG. 4. Estimate of the unoccupied partial DOS (PDOS) of Ni_3^- in the binding-energy range from 0 eV to 1.3 eV assuming a single-particle picture. (a) Resonant 2PPE spectrum (1.5 and 3 eV) of Ni_3^- at a delay 140 fs. Between 1.3 eV and 3 eV the electron intensity results from single-photon photoemission (1PPE). The two-photon electron intensity below 1.3 eV binding energy reflects the *joint density of states*. The dotted line is the 1PPE spectrum shifted by the amount of the pump-photon energy. Dividing the 2PPE spectrum by the dotted spectrum provides the unoccupied partial DOS in (b).

tron lifetime below) and the photoemission probability and the DOS above the vacuum level are assumed to be constant. As the occupied level density $g(E_i)$ is experimentally known from the direct photoemission spectrum the unoccupied partial DOS (PDOS) can be inferred by dividing the 2PPE spectrum by the excitation-energy shifted 1PPE spectrum [dotted line in Fig. 4(a)]. This PDOS $|M_{ni}|^2 g(E_n = E_i + \hbar\omega)$ is shown in Fig. 4(b). From 1.3 eV to 0.9 eV the unoccupied PDOS is nearly constant which explains the similarity between the shifted 1PPE spectrum and the JDOS. The strong decrease of the PDOS between 0.9 eV and 0.5 eV may be caused by a breakdown of the *d*-level density. The distribution between 0.5 eV and 0 eV should not be taken too serious as it is deduced from very low electron intensities.

In order to deduce a mean scattering time τ_{e-e} from our data the evolution of the partial electron intensity in the binding energy range between 0 eV and 0.8 eV has been analyzed [see Fig. 5(a)]. It is assumed that the intensity in this energy range represents an electron population which is initially created by the pump pulse. Due to the natural lifetime, the excited electrons undergo a simple exponential decay with a mean time constant τ_{e-e} for the electrons in the regarded excitation energy range. This assumption is justified by the fact that electrons most likely release half their excitation energy in a single scattering event,²⁹ leading to the removal of the electron from the considered energy range. Moreover, secondary electrons are not expected to contribute significantly in that area.

As the initial excitation by the pump pulse takes place coherently the photoelectron dynamics in Fig. 5(a) can math-

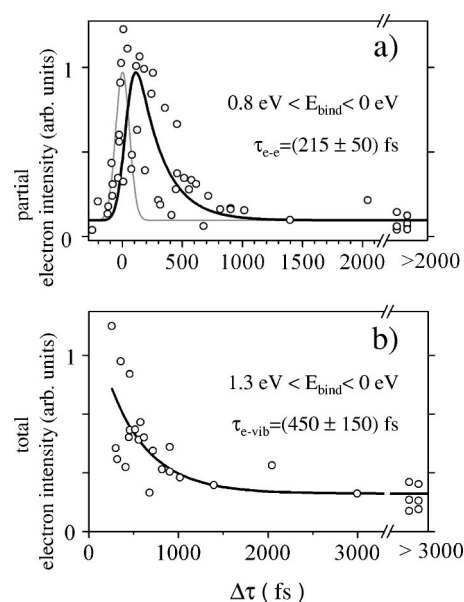


FIG. 5. (a) Population dynamics of the highest excited electrons in the binding energy interval 0–0.8 eV. Using the optical Bloch equations (Ref. 30) a scattering time τ_{e-e} for inelastic electron-electron scattering is deduced for the initially excited electrons in the regarded energy range. The gray line shows the calculated cross correlation curve (the pulse width of pump and probe pulse is 80 fs). (b) The total photoelectron yield (0–1.3 eV above the HOMO) as a function of the delay.

ematically be modeled by the optical Bloch equations for a two-level system.^{30,31} Here the lower level $|1\rangle$ corresponds to the ground level. To consider the relaxation of the excited electrons in the optically excited level $|2\rangle$ a phenomenological relaxation time is introduced which corresponds to a mean inelastic electron lifetime τ_{e-e} . The lifetimes for all levels in the regarded energy range are assumed to be the same. The probing of the electron population by the second pulse is taken into account by convoluting the transient level occupation with the probe pulse intensity function. Applying this model to the experimental data in Fig. 5(a) a mean inelastic electron-electron-scattering time of $\tau_{e-e} = (215 \pm 50)$ fs is found in a least-squares fit.

Moreover, an analysis of the *total* electron intensity above the HOMO (i.e., in the binding-energy range from 1.3 to 0 eV) provides an estimate for a mean electron-vibrational coupling time τ_{e-vib} in Ni_3^- [see Fig. 5(b)]. As the *total* electron intensity above the HOMO is a measure of the excitation energy contained in the electronic system, its decrease with increasing delay indicates how much energy has already drained off into nuclear motion by the coupling of the electronic and nuclear systems. The experimental data have been analyzed for delays beyond 250 fs where a temporal overlap of the pump and probe pulses can be neglected and hence the excitation process need not be considered. Assuming a simple exponential decay for the data in Fig. 5(b) an electron-vibrational coupling time of $\tau_{e-vib} = (450 \pm 150)$ fs is deduced by a least-squares fit.

Similar time-resolved measurements have been performed for the remaining trimer anions of the nickel group.^{17,18} τ_{e-e}

has been determined to (42 ± 19) fs for Pd_3^- and <70 fs for Pt_3^- . Altogether, these results underline that relaxation of optically excited electrons via inelastic electron scattering on a 10–100 fs time scale is characteristic for small transition-metal clusters. As the electronic properties and hence the specific electronic lifetimes for few-atom clusters dramatically fluctuate with the number of atoms as well as the excitation energy it is difficult to relate the particular lifetimes to a periodic trend in the nickel group. The shorter lifetimes of Pd_3^- and Pt_3^- are consistent with the increasing relative size of the d orbitals from the first to the third row of the nickel group which causes an enhanced spatial overlap of the d orbitals and therefore an increase of the electron interaction.

IV. SUMMARY

The ultrafast relaxation of excited electrons via inelastic electron-electron scattering in isolated Ni_3^- clusters has been observed in a two-color pump-probe experimental setup ($h\nu=1.5$ and 3 eV). Using the optical Bloch equations a

series of time resolved background-free photoelectron spectra reveal a mean lifetime of $\tau_{e-e}=(215 \pm 50)$ fs for electrons initially excited between 0 and 0.8 eV binding energy. Assuming a simple exponential decay for the total hot electron intensity an electron-vibrational coupling time of $\tau_{e-vib}=(450 \pm 150)$ fs has been deduced. The mean number of excited states in a three-atom transition-metal cluster has been estimated to be two orders of magnitude larger than in a noble-metal cluster. This explains why inelastic electron scattering can be observed in transition-metal clusters but not in small s/p -metal clusters.

ACKNOWLEDGMENTS

We thank A. Bringer, Forschungszentrum Jülich GmbH, for stimulating and valuable discussions. V. Stert, Max Born Institute, Berlin, is furthermore acknowledged for providing a computer program to solve the Bloch equations. We thank D. Henkel, Forschungszentrum Jülich GmbH, for fitting support.

-
- ¹P. Grünberg, R. Schreiber, Y. Pang, M. Brodsky, and H. Sowers, *Phys. Rev. Lett.* **57**, 2442 (1986).
- ²H. Petek, M. J. Weida, H. Nagano, and S. Ogawa, *Science* **288**, 1402 (2000).
- ³E. Beaupaire, J.-C. Merle, A. Daunois, and J.-Y. Bigot, *Phys. Rev. Lett.* **76**, 4250 (1996).
- ⁴M. Aeschlimann, M. Bauer, and S. Pawlik, *Chem. Phys.* **205**, 127 (1996).
- ⁵E. Knoesel, A. Hotzel, T. Hertel, M. Wolf, and G. Ertl, *Surf. Sci.* **368**, 76 (1996).
- ⁶H. Petek and S. Ogawa, *Prog. Surf. Sci.* **56**, 239 (1997).
- ⁷J.-Y. Bigot, V. Halté, J.-C. Merle, and A. Daunois, *Chem. Phys.* **251**, 181 (2000).
- ⁸J. H. Hodak, I. Martini, and G. V. Hartland, *J. Phys. Chem. B* **102**, 6958 (1998).
- ⁹S. Link and M. A. El-Sayed, *J. Phys. Chem. B* **103**, 8410 (1999).
- ¹⁰C. Voisin, D. Christofilos, N. Del Fatti, F. Vallée, B. Prével, E. Cottancin, J. Lermé, M. Pellarin, and M. Broyer, *Phys. Rev. Lett.* **85**, 2200 (2000).
- ¹¹J. Ho, K. M. Ervin, and W. C. Lineberger, *J. Chem. Phys.* **93**, 6987 (1990).
- ¹²K. M. McHugh, J. G. Eaton, G. H. Lee, H. W. Sarkas, L. H. Kidder, J. T. Snodgrass, M. R. Manaa, and K. H. Bowen, *J. Chem. Phys.* **91**, 3792 (1989).
- ¹³K. J. Taylor, C. L. Pettiette-Hall, O. Cheshnovsky, and R. E. Smalley, *J. Chem. Phys.* **96**, 3319 (1992).
- ¹⁴T. Baumert, R. Thalweiser, and G. Gerber, *Chem. Phys. Lett.* **209**, 29 (1993).
- ¹⁵G. Ganteför, S. Kraus, and W. Eberhardt, *J. Electron Spectrosc. Relat. Phenom.* **88-91**, 35 (1998).
- ¹⁶D. Ievlev, I. Rabin, W. Schulze, and G. Ertl, *Chem. Phys. Lett.* **328**, 142 (2000).
- ¹⁷N. Pontius, P. S. Bechthold, M. Neeb, and W. Eberhardt, *Phys. Rev. Lett.* **84**, 1132 (2000).
- ¹⁸N. Pontius, G. Lüttgens, P. S. Bechthold, M. Neeb, and W. Eberhardt, *J. Chem. Phys.* **115**, 10 479 (2001).
- ¹⁹G. Lüttgens, N. Pontius, P. S. Bechthold, M. Neeb, and W. Eberhardt, *Phys. Rev. Lett.* **88**, 076102 (2002).
- ²⁰N. Pontius, P. S. Bechthold, M. Neeb, and W. Eberhardt, *Appl. Phys. B: Lasers Opt.* **71**, 351 (2000).
- ²¹G. Ganteför and W. Eberhardt, *Phys. Rev. Lett.* **76**, 4975 (1996).
- ²²K. M. Ervin, J. Hoe, and W. C. Lineberger, *J. Chem. Phys.* **89**, 4514 (1988).
- ²³In this paper the term “above the HOMO” means at “lower binding energies with respect to the HOMO” and “below the HOMO” “at higher binding energies with respect to the HOMO.” The term ‘binding energy’ is used in the context of a single particle picture and generally refers to a *single*-photon photoemission process. It therefore corresponds to the common terminology in photoemission spectroscopy. For two-photon photoemission involving a resonant intermediate state the term refers to the second single-photon photoemission process. Here the photoemission does not occur from the ground state but from an (photo)excited state. That is why here emitted electrons can have lower binding energies than that of the HOMO.
- ²⁴Within the single-particle picture the binding energy of the HOMO equals the ionization potential. Considering an absolute uncertainty of the electron spectrometer calibration of 100 meV the extracted value of 1.3 eV is consistent with the results in Ref. 21.
- ²⁵D. E. Ellis, J. Guo, H.-P. Cheng, and J. J. Low, *Adv. Quantum Chem.* **22**, 125 (1991).
- ²⁶P. T. Dinda, G. V. Tsinganos, N. Flytzanis, and A. D. Mitrionis, *Phys. Rev. B* **51**, 13 697 (1995).
- ²⁷N. Watari and S. Ohnishi, *Phys. Rev. B* **58**, 1665 (1998).
- ²⁸M. Moseler, H. Häkkinen, R. N. Barnett, and U. Landman, *Phys. Rev. Lett.* **86**, 2545 (2001).
- ²⁹J. J. Quinn, *Phys. Rev.* **126**, 1453 (1962).
- ³⁰R. Loudon, *The Quantum Theory of Light* (Oxford University Press, New York, 1983).
- ³¹Th. Freudenberg, W. Radloff, H.-H. Ritze, V. Stert, K. Weyers, F. Noak, and I. V. Hertel, *Z. Phys. D: At., Mol. Clusters* **36**, 349 (1998).